



Lithiation/Delithiation Performance of Cu_6Sn_5 with Carbon Paper as Current Collector

Catia Arbizzani,* Mariachiara Lazzari, and Marina Mastragostino*^z

University of Bologna, Unità Complessa di Istituti di Scienze Chimiche, Radiochimiche e Metallurgiche,
40127 Bologna, Italy

Lithiation/delithiation of Cu_6Sn_5 both electrochemically and mechanochemically prepared on a carbon paper (CP) current collector was investigated by repeated galvanostatic cycles with time-limited charges to insert different amounts of lithium per Sn atom (Li/Sn) into the alloy. The results demonstrated that, unlike Cu_6Sn_5 electrodeposited on Cu foil, both electrochemical and mechanochemical Cu_6Sn_5 on CP can undergo hundreds of lithiation/delithiation cycles with Li/Sn > 2 at high current density (0.74 mA cm^{-2}), thereby delivering constant amounts of charge with coulombic efficiency near 100%. The Cu_6Sn_5 /CP electrodes with a loading of 6.6 mg cm^{-2} and charge limited to 2.43 Li/Sn yielded a specific capacity of 330 mAh g^{-1} and a capacity per geometric area of 2.18 mAh cm^{-2} . These values compare well with those of graphite-based anodes of commercial batteries. The significant improvement in cyclability performance of the Cu_6Sn_5 /CP electrodes is due to the CP current collector's three-dimensional conductive matrix, which preserves the electric contact over cycling so that alloy cracking becomes less detrimental for the electric contact.

© 2004 The Electrochemical Society. [DOI: 10.1149/1.1839466] All rights reserved.

Manuscript submitted March 30, 2004; revised manuscript received June 23, 2004. Available electronically December 20, 2004.

Lithium-ion battery technology is well consolidated in the field of portable equipment.¹ Nevertheless, research efforts in the lithium-ion battery field have been exceedingly active in attempts to ameliorate the performance of these devices in terms of electrode materials, electrolyte media, and design. For negative electrodes, the research is mainly focused in two directions: (i) the optimization of the performance of carbonaceous materials,²⁻⁵ and (ii) the search for alternative materials to the carbonaceous ones presently used, which has led to the development of metal oxides^{6,7} and metal alloys.⁸ While Li/metal alloys are very attractive for their specific capacity, their high volume change, which is related to the insertion/removal of lithium, causes pulverization of the electrode and, hence, loss of electrical contact among particles, which is responsible for the poor cycle life. For example, tin can sustain only a few charge/discharge cycles before losing structural integrity, even when the charge is limited to 1.5 Li/Sn atomic ratio.⁹ Several strategies to reduce this problem have been pursued, including the preparation of superfine and nanometric materials, intermetallic compounds, and alloy/carbon composites, but none has been decisive.¹⁰⁻¹⁵

While the relationship between morphology and electrochemical properties of alternative materials to graphite and of graphite itself has been under study,^{14,16-18} minor studies have been devoted to the nature and morphology of current collectors. Recently, Fujitani *et al.*^{13,19} demonstrated the effect of the surface roughness of copper foil, the current collector generally used for the negative electrode, on improving cyclability data. This improvement is attributed to the formation of a microcolumnar structure of the deposits, which cracks periodically in accordance with the surface profile of the Cu rough foil, providing spaces for the active material to swell either upwards or sideways during charge. By contrast, flat surfaces crack randomly, so that the active material pulverizes and delaminates from the foil.

We focus on the electrochemical stability of Cu_6Sn_5 . The Cu_6Sn_5 shows structural compatibility with its lithiated phase $\text{Li}_x\text{Cu}_6\text{Sn}_5$ ($0 < x < 13$), which is isostructural with Li_2CuSn , so that the sublattice of Sn, which is the active component of the intermetallic compound, suffers moderate distortion in the lithiated phase.²⁰ In addition, the Cu inactive matrix buffers the Sn volume changes accompanying the reactions with Li, whereas Sn alone reaches a volume expansion of up to 300% when 4.4 Li per Sn atom are inserted.²¹ However, Cu_6Sn_5 displays a volume expansion of

148% with the same degree of lithiation and an expansion of only 59% when 2 Li are reversibly inserted to give Li_2CuSn , according to the following reactions^{22,23}



The lithiation of Cu_6Sn_5 as in Reaction 2 occurs at 0.4 V vs. Li. This potential value is an important feature of Cu_6Sn_5 , because, in lithium-ion batteries using flammable organic electrolytes, anode materials in which the lithiation process starts at a more positive potential than in graphite are required to avoid the risk of Li metal deposition. The theoretical specific capacity of Cu_6Sn_5 was estimated to be 358 mAh g^{-1} (a value near that of graphite) when lithiated to the composition $\text{Li}_{13}\text{Cu}_6\text{Sn}_5$, *i.e.*, when the Li/Sn atomic ratio is 2.6.²⁴ Until now the cycling stability of Cu_6Sn_5 on conventional metal current collectors (Cu, Ni) has not been satisfactory because the volume changes, still present, and the Cu extrusion lead to a loss of electric contact among particles and delamination from the current collectors.

We examined commercial carbon paper (CP) as a new current collector for Cu_6Sn_5 negative electrodes for lithium-ion batteries. CP is a porous material of high electrical conductivity and used as a substrate/electrode in electrochemical devices like supercapacitors and fuel cells capable of sustaining high currents per geometric area. CP may be a suitable current collector for metals or intermetallic compounds because it is a conducting three-dimensional matrix that can host them, not only on the surface but also inside it, and it can buffer the volume changes of the hosted material. While CP might be involved in the electrochemical processes of lithiation/delithiation, the advantage of Sn/carbonaceous materials composites over Sn has been demonstrated.^{11,12} Electrodes of Cu_6Sn_5 electrodeposited on CP and on Cu and of mechanochemical Cu_6Sn_5 permeated through CP from a suspension (Cu_6Sn_5 96 wt % and poly(vinylidene fluoride) 4 wt %) in acetone were subjected to repeated lithiation/delithiation galvanostatic cycles with time-limited charges to insert different amounts of lithium, and the results using the two current collectors are compared and discussed.

Experimental

Cu-Sn alloys were galvanostatically deposited on copper foils (25 μm thick) and CP (Spectracorp 2050, 10 mils) sheets, both pretreated in acid solution, from a 0.1 M SnCl_2 -0.025 M CuSO_4 -0.5

* Electrochemical Society Active Member.

^z E-mail: marina.mastragostino@unibo.it

M H₂SO₄ degassed solution at room temperature. Adhesive tape was used to prevent deposition on the back of the electrode and to limit the exposed area to 1 cm². Ultrapure water (Milli-Q, 18.6 MΩ cm, Simplicity Water System, Millipore Co.) was employed for solutions and rinsing. Electrodes with different amounts of Cu-Sn intermetallic compound (2-6 mg cm⁻²) were prepared at constant current (-12 mA cm⁻²). As the efficiency of the electrodeposition was low, alloy mass loading was evaluated by weighing. The potential during galvanostatic electrodeposition was *ca.* -0.5 V vs. saturated calomel electrode. The electrodes were dried under vacuum at 60°C for 16 h before use. Nanometric η'-Cu₆Sn₅ (Sn 45.5, Cu 54.5 atom %) prepared mechanochemically was also used to prepare electrodes by permeation of a suspension of Cu₆Sn₅ (96 wt %), poly(vinylidene fluoride) (4 wt %), and acetone through CP sheets. These electrodes, with a Cu₆Sn₅ mass loading of 3-14 mg cm⁻², were dried 1 h at 70°C under vacuum at room temperature before use.

All the electrodes were characterized by X-ray diffraction (XRD) analysis with a Philips PW1050/81 powder diffractometer (Cu Kα radiation, 40 mA, 40 kV). Scanning electron microscopy (SEM) analyses were performed with a Philips 515 SEM microscope equipped with an EDAX PV9900 energy dispersion detector for X-ray energy-dispersive spectroscopy (EDS). For secondary electron imaging and for EDS, 20 and 25 keV electrons were used. The particle/aggregate dimensions were measured with a Fritsch Analysette 22 Compact laser particle sizer in the range 0.3-300 μm (62 channels) with 5 scans/measurement.

All the electrodes were electrochemically characterized by galvanostatic charge/discharge cycles at $T = 30 \pm 1^\circ\text{C}$ in a T-shaped cell sealed in a dry box (Mbraun Labmaster 130, O₂ and H₂O < 1 ppm). The working electrodes were cut with a hollow brass punch. Due to the resharpening of the punch's rim, the area was $0.68 \pm 0.02\text{ cm}^2$. Given the inhomogeneous density of the CP sheets, the masses of the CP current collectors, evaluated by weighing, are reported in all the figures related to electrochemical measurements. The counter electrode was metallic Li in excess, and the reference electrode for monitoring the electrode potentials was a Li foil. The separator, a Whatman GF/D glass fiber disk, was imbibed with the electrolyte solution ethylene carbonate:dimethyl carbonate (EC:DMC2:1)-1 M LiPF₆ (LP31 Merck, battery grade). The galvanostatic cycles were carried out at 0.500 mA, *i.e.*, $0.74 \pm 0.02\text{ mA cm}^{-2}$. The terms "charge" and "discharge" refer to the alloy electrode being used as the anode in lithium-ion batteries, *i.e.*, to lithiation and delithiation, respectively. The discharges were potential limited (2.000 V vs. Li), and the charges were time limited (while maintaining a safe voltage cutoff of 0.005 V vs. Li) to insert defined amounts of lithium per atom of tin. The amount of lithium to be inserted (estimated as the product of current and time) was calculated, in relation to the Li/Sn atomic ratio to be reached, on the basis of the mass of the Cu₆Sn₅ loaded on the electrode. The specific capacity of Cu₆Sn₅ was calculated by assuming that all the lithiation charge involved the Cu₆Sn₅. The cells with electrodes having high alloy mass loading were disassembled and reassembled to change the Li metal counter electrode (and in some cases even the separator) after a certain number of cycles, *i.e.*, when the sum of their charges was *ca.* 400 C cm⁻², to prevent the Li metal deposition/dissolution at the counter electrode from interfering with the cycling stability of the Cu₆Sn₅. The electrochemical deposition and characterization were performed with a VMP multichannel potentiostat and a PAR 273A potentiostat/galvanostat.

Results and Discussion

We started with the electrochemical synthesis of Cu₆Sn₅ on both CP and Cu current collectors. Given that the copper electrodeposition potential is less negative than that of tin, a solution with a concentration of tin higher than that of copper was selected for the galvanostatic electrodeposition of the Cu-Sn intermetallic compound. The SEM photographs at different magnification of CP in Fig. 1a,b show an open and fibrous structure (fiber diam *ca.* 10 μm)

that can host active materials. SEM images of the electrochemical Cu_xSn_y compound on CP in Fig. 1c,d show the CP fibers homogeneously covered with Cu_xSn_y. The covering appears to be particles and aggregates of different sizes (the smallest are <1 μm), the biggest having a leaf shape. Figure 1e,f displays the SEM images of mechanochemical Cu₆Sn₅ on CP and mechanochemical Cu₆Sn₅ powder. Here the Cu₆Sn₅ deposited on CP by permeation is more localized where the fibers criss-cross, but it is present in the whole volume of CP (as per SEM images, not shown, of the back side of the Cu₆Sn₅/CP electrodes). Most of the carbon fibers remained bare, and the aggregates of different sizes are made of nanometric particles. Figure 2 displays the "particle" size distribution of the mechanochemical Cu₆Sn₅. The abscissa is the particle or, as in our case, the agglomerate size, which can be viewed as an "equivalent diameter," *i.e.*, the diameter of a sphere which exhibits the same physical properties as the measured, irregular particle or agglomerate. The ordinate is the oversize cumulative distribution indicating the total quantity of all agglomerates with equivalent diameter smaller than or equal to the abscissa value. The size of 90% of the agglomerates is <20 μm.

Figure 3 shows the XRD patterns of different electrodes: bare CP, electrochemical Cu_xSn_y/CP, and mechanochemical Cu₆Sn₅/CP; the pattern of Sn electrodeposited on CP is also reported for comparison. The figure also indicates the main reflections of the different materials (stars for the Cu₆Sn₅ and circles for the Sn main peaks). The electrochemical Cu_xSn_y, unlike the pattern of mechanochemical Cu₆Sn₅, shows the coexistence of two phases, η'Cu₆Sn₅ and Sn. While the reflections attributable to tin oxides or copper oxides are absent in both the (b) and (c) spectra, the reflections of CP are recognizable in all the spectra. From the EDS analysis of several portions of an electrochemical Cu_xSn_y/CP, we estimated a mean value for the Cu/Sn atomic ratio of 1.19 ± 0.11 , and we considered it reasonable to take the electrodeposited material as Cu₆Sn₅.

Cu₆Sn₅ was electrodeposited on both Cu and CP. As the efficiency of the electrodeposition process was low, we considered the increase of the electrode weight instead of the charge involved in the electrodeposition to evaluate alloy mass loading. We first tested electrodes with a Cu₆Sn₅ mass loading of *ca.* 4-6 mg cm⁻². The coulombic efficiency of the first galvanostatic cycle of Cu₆Sn₅ both on Cu and CP ranged from 60 to 75%, being affected, just like the carbonaceous materials, by irreversible capacity due to side reactions at the electrode/electrolyte interface. Figure 4 reports the voltage profiles of repeated galvanostatic charge/discharge cycles of Cu₆Sn₅ on copper, where the charge process was time limited to insert lithium up to 1.88 Li/Sn atomic ratio. However, after the first three cycles, in which the lithiation plateau at 0.4 V progressively disappeared, the potential of the Cu₆Sn₅/Cu electrode reached the charge cutoff voltage (5 mV), and the amount of Li inserted (and deinserted) became lower and lower than the 1.88 atom per Sn. Figure 5 displays the discharge capacity from galvanostatic cycles of two Cu₆Sn₅/Cu electrodes of the same area with initial charges further limited to 1.10 Li/Sn and 0.59 Li/Sn. In these cases, too, the alloy electrode's stability was low, as well as its coulombic efficiency. The reason for this decay can be found in the formation of cracks, as also reported in the literature.¹³ The Cu foil cannot support the stress of the Cu-Sn alloy during the lithiation/delithiation, which results in pulverizing and delaminating from the Cu foil of the material, with cracks up to 20 μm wide, as we observed by SEM of the electrodes after 100 cycles. The low coulombic efficiency may also lead to electrode material pulverization, which produces new surface area able to react with the electrolyte, in addition to interparticle contact loss.¹⁶

Figure 5 also reports the capacity data from galvanostatic cycles of a Cu₆Sn₅/CP electrode, which indicate that the use of the CP current collector is successful when compared to that of Cu. The

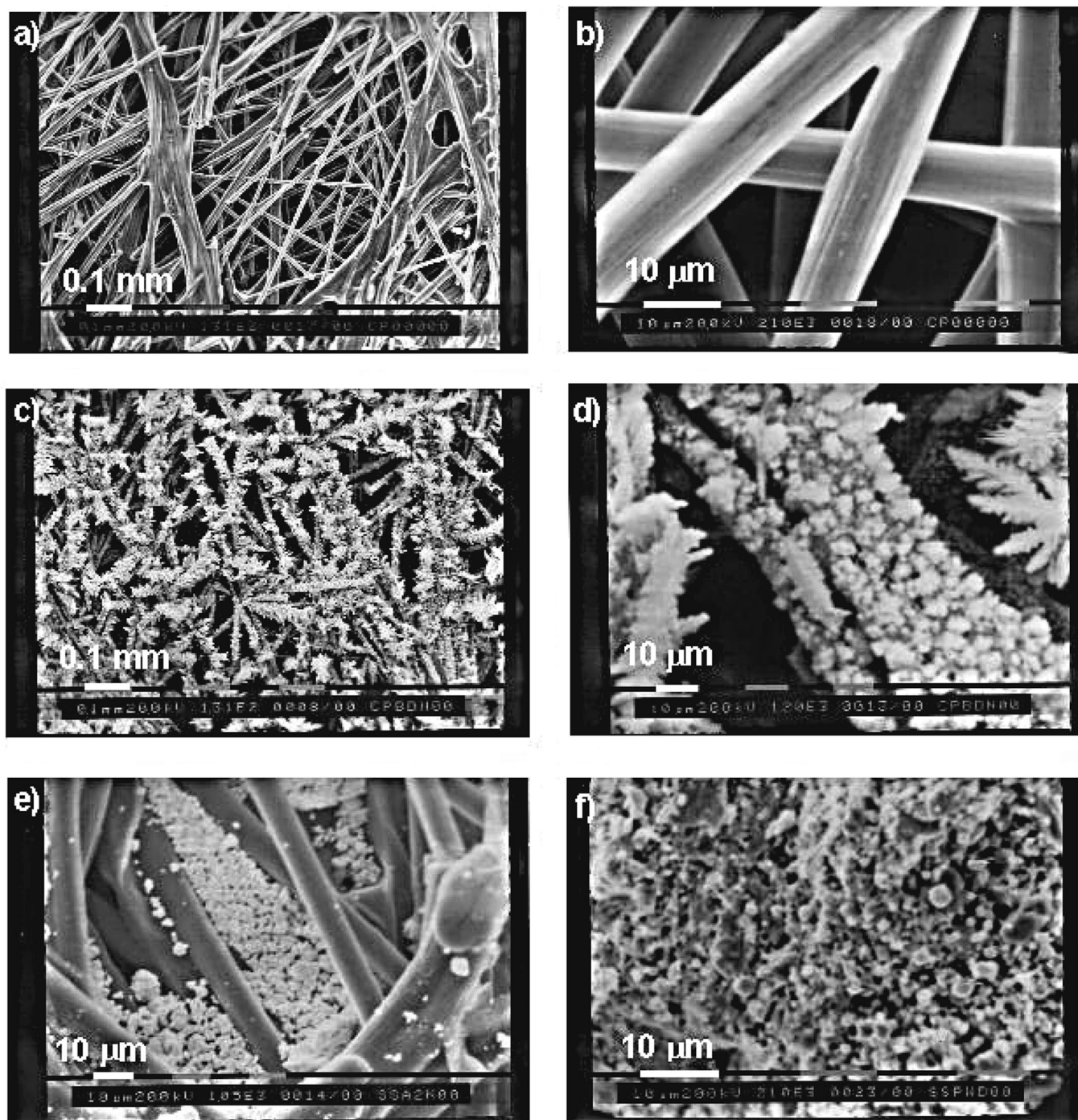


Figure 1. SEM images of bare CP with (a) 131 times and (b) 2100 times magnification, of electrochemical $\text{Cu}_6\text{Sn}_5/\text{CP}$ with (c) 131 times and (d) 1200 times magnification, and of (e) mechanochemical $\text{Cu}_6\text{Sn}_5/\text{CP}$ with 1050 times magnification, and (f) mechanochemical Cu_6Sn_5 powder with 2100 times magnification.

$\text{Cu}_6\text{Sn}_5/\text{CP}$ electrodes display high reproducibility and high cycling stability over 250 cycles, with coulombic efficiency near 100% both when the charge is limited to 1.44 Li/Sn and 1.84 Li/Sn, and the maximum specific capacity of the $\text{Cu}_6\text{Sn}_5/\text{CP}$ electrode in Fig. 5 is 253 mAh g^{-1} .

Figure 6 displays the voltage profiles of galvanostatic cycles of the electrochemical $\text{Cu}_6\text{Sn}_5/\text{CP}$ electrode in Fig. 5 with time-limited charges compared to the galvanostatic charge/discharge cycles at the same current of bare CP current collector (0.68 cm^2) with the time-limited charge set to 1 h 30 min (Fig. 6a,b) and 2 h (Fig. 6c). For the $\text{Cu}_6\text{Sn}_5/\text{CP}$ electrode, the plateau of lithiation at

0.4 V progressively decreases in length. After 40 lithiation/delithiation cycles, the voltage profiles are smoothed, and none of them reached the charge cutoff potential of 5 mV even when the charge time was increased to 1 h 55 min (Fig. 6c). The voltage profiles of bare CP at different cycle numbers and different time-charge settings clearly indicate that CP can also be lithiated and delithiated, the process being reversible with high coulombic efficiency (near 100%) with the exception of the very first cycles. The coulombic efficiency of the first cycle of different CP electrodes ranged from 70-85%, indicating that CP even displays the irreversible capacity due to side reactions at the electrode/electrolyte inter-

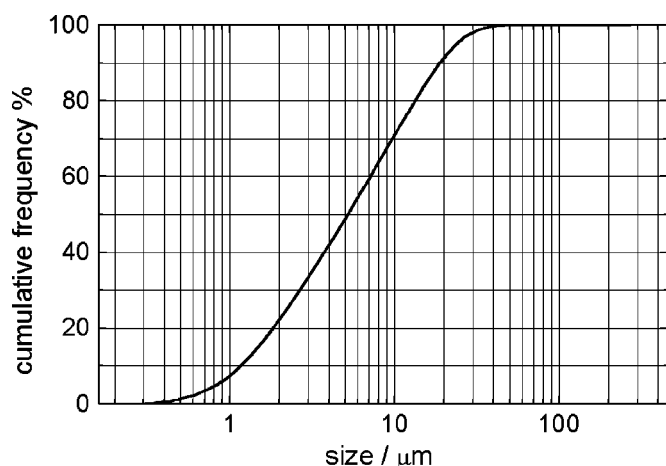


Figure 2. Agglomerate size distributions of mechanochemical Cu_6Sn_5 .

face. However, the lithiation process at the CP electrodes occurs at lower potentials than that at $\text{Cu}_6\text{Sn}_5/\text{CP}$, and with time-limited charges set to 2 h the cutoff potential of 5 mV was reached after 40 cycles and the charge time of the 120th cycle became less than 1 h. The specific capacity of CP was 140 mAh g^{-1} for the first 40 cycles, but it decreased sharply and reached 65 mAh g^{-1} after 150 cycles. All of this suggests that the lithiation process of $\text{Cu}_6\text{Sn}_5/\text{CP}$ electrodes is mainly due to the Cu_6Sn_5 , and the role which may be ascribed to CP is that of an excellent three-dimensional current collector. The evolution of the voltage profiles of the $\text{Cu}_6\text{Sn}_5/\text{CP}$ electrode over a hundred cycles is due to a deterioration of the crystalline structure of the alloy by gradual pulverization (also shown by a slight decrease in the intensity of the characteristic peaks in XRD patterns, not reported here). However, it does not result in capacity loss because of the CP's ability to prevent loss of electrical contact with the active material. Even a low crystalline alloy hosted in the three-dimensional CP current collector thus retains lithium insertion capability.

To increase specific capacity, we carried out galvanostatic charge/discharge cycles of $\text{Cu}_6\text{Sn}_5/\text{CP}$, where the charges were time-limited to $\text{Li}/\text{Sn} > 2$; so as not to overly affect the measurement time, we also tested electrodes with Cu_6Sn_5 mass loading $< 3 \text{ mg cm}^{-2}$. The capacity values of both electrochemical and mechanochemical $\text{Cu}_6\text{Sn}_5/\text{CP}$ electrodes with time-limited charges for

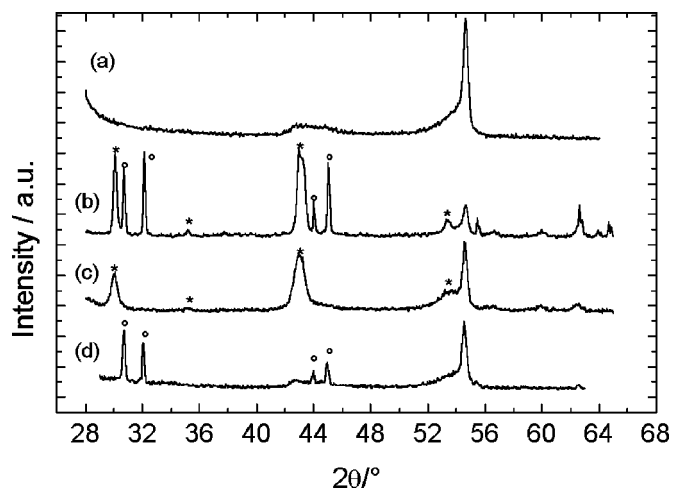


Figure 3. XRD patterns of (a) bare CP, (b) electrochemical $\text{Cu}_6\text{Sn}_5/\text{CP}$, (c) mechanochemical $\text{Cu}_6\text{Sn}_5/\text{CP}$, and (d) Sn/CP electrodes.

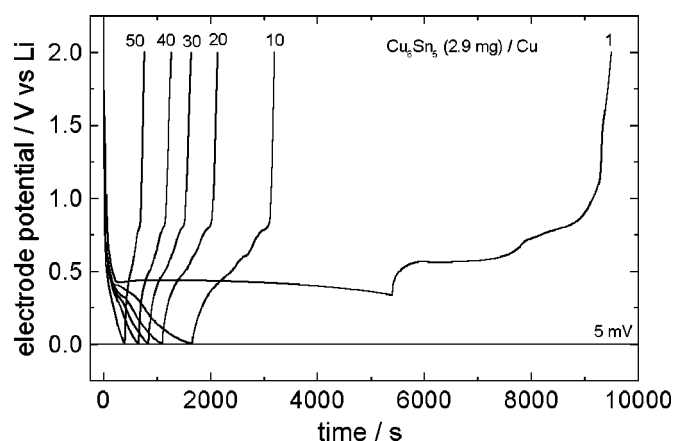


Figure 4. Voltage profiles of different galvanostatic charge/discharge cycles at 0.500 mA of electrochemical Cu_6Sn_5 (2.9 mg per 0.68 cm^2) on Cu foil. The initial lithium insertion was 1.88 Li/Sn mol ratio.

amounts of inserted Li up to 3.65 Li/Sn are reported in Fig. 7. These electrodes were stable over 260 cycles and never reached the charge cutoff potential of 5 mV; the maximum specific capacity estimated by the electrodes with light alloy mass loading is *ca.* 500 mAh g^{-1} . The comparison of the voltage profiles of the light-loaded $\text{Cu}_6\text{Sn}_5/\text{CP}$ electrodes and of bare CP seems to suggest an important contribution of the lithiation of CP during the charge process of the alloy, but only at the first tens of cycles.

To verify the possibility of increasing the capacity per geometric area of the $\text{Cu}_6\text{Sn}_5/\text{CP}$ electrodes with high alloy mass were prepared using mechanochemical Cu_6Sn_5 , given that the electrochemical deposition provided at maximum a mass loading of 4 mg. Figure 8a displays the capacity per geometric area of mechanochemical $\text{Cu}_6\text{Sn}_5/\text{CP}$ electrodes with mass loading from 5.1 to 6.8 mg of Cu_6Sn_5 and with the galvanostatic charges limited to a 2.02-2.08 Li/Sn ratio. It is evident from this figure that $\text{Cu}_6\text{Sn}_5/\text{CP}$ can sustain a high number of galvanostatic cycles at high current density, delivering a capacity of up to 2.85 mAh cm^{-2} with a specific capacity of *ca.* 285 mAh g^{-1} of Cu_6Sn_5 for all the tested electrodes. Electrodes with a higher mass loading (9.5 mg) were also tested. While we observed capacity values of 3.90 mAh cm^{-2} (corresponding to *ca.*

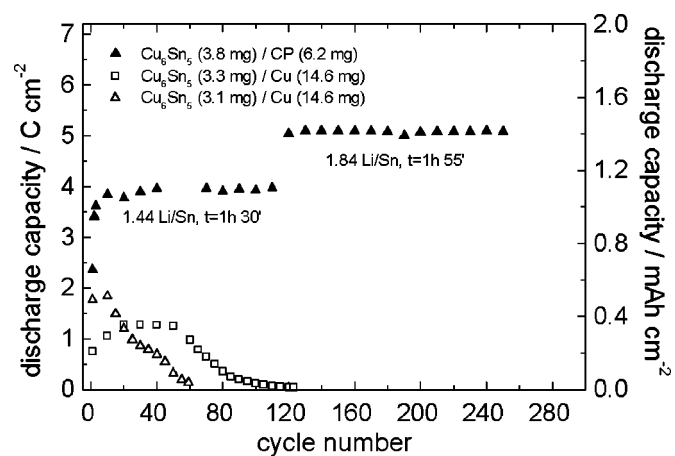


Figure 5. Discharge capacity from galvanostatic charge/discharge cycles at 0.500 mA per 0.68 cm^2 of electrochemical $\text{Cu}_6\text{Sn}_5/\text{CP}$ and $\text{Cu}_6\text{Sn}_5/\text{Cu}$ at different amounts of lithium inserted. The Li/Sn mol ratio, time of charge for $\text{Cu}_6\text{Sn}_5/\text{CP}$, and the mass of Cu_6Sn_5 and CP are indicated. For $\text{Cu}_6\text{Sn}_5/\text{Cu}$ electrodes, the initial Li/Sn was 0.59 (empty square) and 1.10 (empty triangles), respectively.

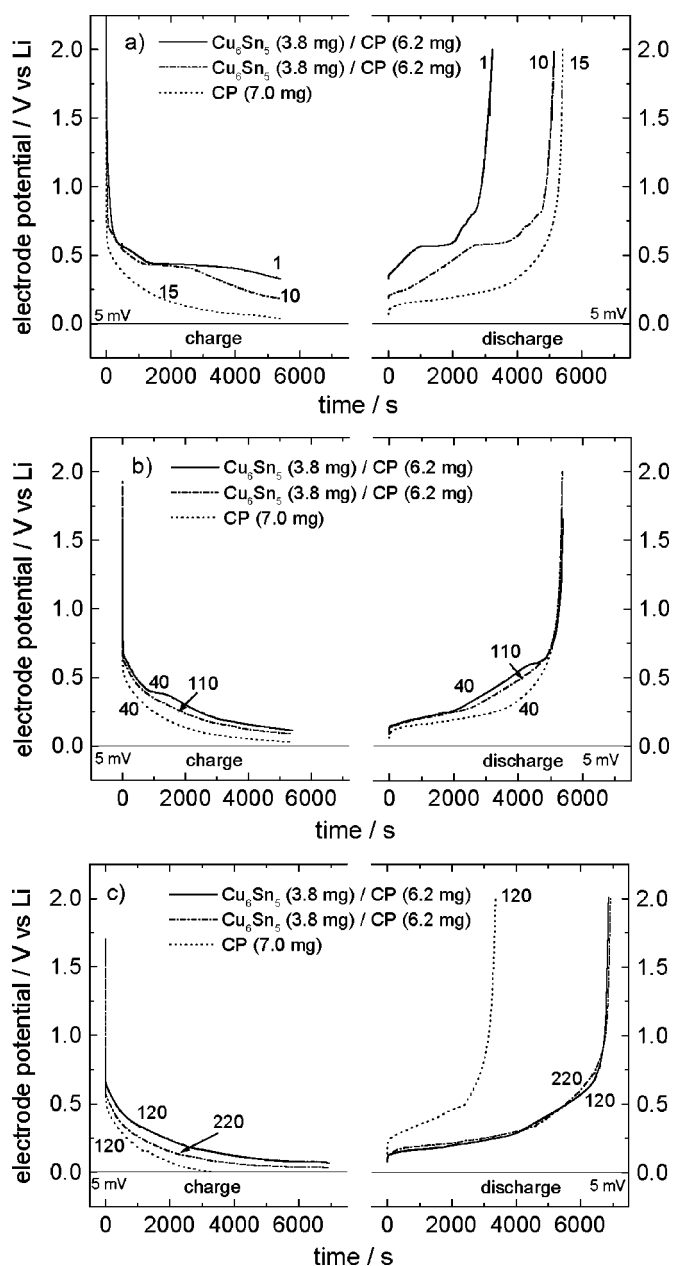


Figure 6. Voltage profiles of galvanostatic charge/discharge cycles at 0.500 mA per 0.68 cm² of electrochemical Cu₆Sn₅ (3.8 mg)/CP and of bare CP (7.0 mg) at different cycle numbers. The charge time was 1 h 30 min (a and b) and 1 h 55 min (c), corresponding to 1.44 and 1.84 Li/Sn mol ratio, respectively. The charge of bare CP was time-limited to 1 h 30 min (a and b) and to 2 h (c). After 40 (2 h) cycles, the charge of CP was limited by the cutoff potential (5 mV).

280 mAh g⁻¹ of Cu₆Sn₅), they decreased to half after 100 cycles and remained almost constant up to 200 cycles. There could be two causes for this decrease. The involvement of a high charge per cycle, due to the high alloy mass loading, required several changes of the Li counter electrode, which involved disassembling and reassembling the cell three times during the first 70 cycles; hence, the most superficial alloy may have been removed from the current collector. The second cause could be a more important bulk effect in the electrode with very high mass loading with the alloy that does not draw advantage from the CP support. These results thus indicate a maximum feasible Cu₆Sn₅ mass loading of 10 mg cm⁻² for CP. Figure 8b shows the voltage profiles of the 50th cycle of the

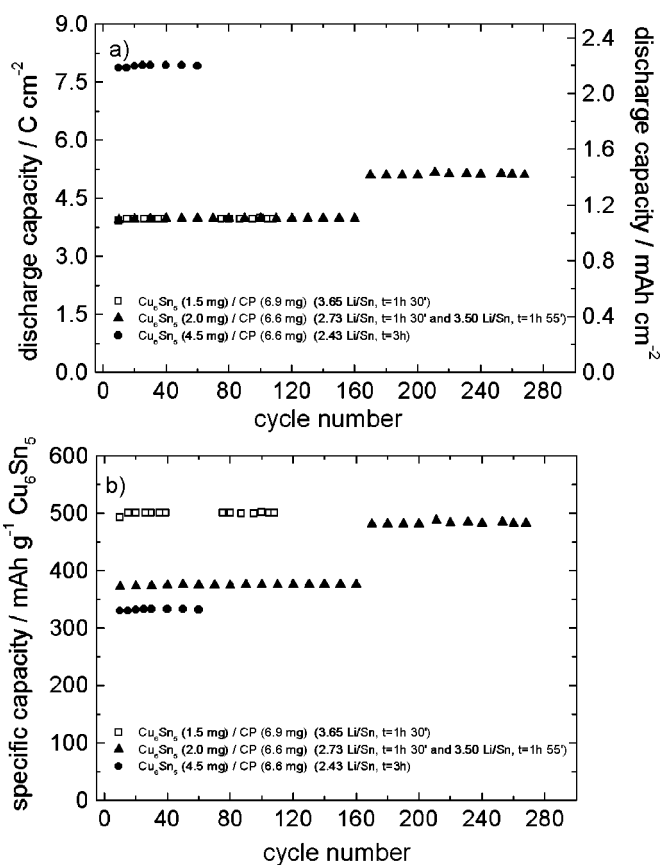


Figure 7. (a) Discharge capacity and (b) specific capacity from galvanostatic charge/discharge cycles at 0.500 mA per 0.68 cm² of electrochemical (empty squares) and mechanochemical (solid triangles and circles) Cu₆Sn₅/CP electrodes at different amounts of lithium inserted. The mass of Cu₆Sn₅ and CP, the Li/Sn value, and the time of charge are indicated.

Cu₆Sn₅/CP electrode (6.8 mg of alloy mass) compared with the 40th cycle of a bare CP electrode. As in Fig. 6, it is evident that the process of lithiation/delithiation is that of Cu₆Sn₅, as its voltage profiles during charge remain at higher voltages than those of CP. In addition, the charge time of these heavy electrodes is always higher than that which the bare CP electrodes can sustain.

The excellent stability performance of the submicrometric Cu₆Sn₅ on CP, both for electrodes with high alloy mass loading up to 10 mg cm⁻² and with lithium insertion Li/Sn > 2 for over 100 cycles, is due to the CP matrix, which ensured a three-dimensional electric contact even if alloy agglomeration and some cracks are visible after 100 cycles, especially on the mechanochemical Cu₆Sn₅.

Conclusions

The results of this study demonstrate that the Cu₆Sn₅ alloy, whether electrochemically prepared directly into the CP or mechanochemically prepared and hosted into it, can undergo hundreds of cycles of lithiation to Li/Sn > 2 and delithiation, delivering constant amounts of charge with coulombic efficiency near 100% after the first few cycles. The cycling test at 0.74 mA cm⁻² of Cu₆Sn₅/CP electrodes with alloy loading of 3 mg cm⁻² and charge-limited to 3.50 Li/Sn provided specific capacity values of 480 mAh g⁻¹. Those of the electrodes with loading of 6.6 mg cm⁻² and charge-limited to 2.43 Li/Sn had specific capacity values of 330 mAh g⁻¹ (and capacity values per geometric area of 10 mg cm⁻² can be estimated), and those with loading of 10 mg cm⁻² and charge limited to 2.08 Li/Sn had capacity values of 285 mAh g⁻¹ (and an estimated capacity value per geometric area of 2.85 mAh

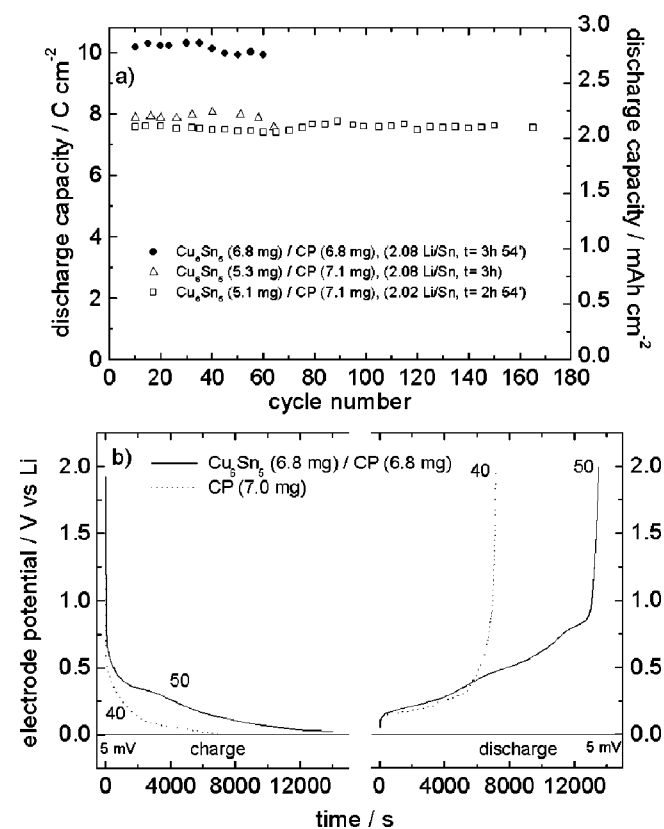


Figure 8. (a) Discharge capacity from galvanostatic charge/discharge cycles at 0.500 mA per 0.68 cm² of mechanochemical Cu₆Sn₅/CP electrodes. The lithium insertion was >2 Li/Sn with time of charge of 3 h 54 min (solid circles), 3 h (empty triangles), and 2 h 54 min (empty squares). The charge cutoff potential of 5 mV was reached after the 60th and the 50th cycles for the electrodes indicated by the solid circles and the empty triangles, respectively. The mass of Cu₆Sn₅ and CP are indicated. (b) Voltage profiles of galvanostatic charge/discharge cycles of mechanochemical Cu₆Sn₅/CP electrode with the charge time-limited to 3 h 54 min and of CP (7.0 mg).

cm⁻²). Given, too, the high current density used in the galvanostatic tests, 330 mAh g⁻¹ and 2.18 mAh cm⁻² are values of particular relevance from a practical point of view. That the Cu₆Sn₅ alloy hosted into CP does not require a carbon-conducting additive, as the graphite anodes generally do, and taking into account the addition of 4 wt % of binder, these capacity values became 317 mAh g⁻¹ of deposited mass and 2.09 mAh cm⁻². These values compare well with the values 358 mAh g⁻¹ and 2.3 mAh cm⁻² of graphite-based anodes of high-performance commercial batteries^{25,26} and have the safety advantage that most of the lithiation process occurs at more positive potentials than in graphite. This comparison is still favorable when the mass of the current collectors is considered, being that CP displays a mass of ca. 10 mg cm⁻², a value lower than those of the Cu foils of commercial batteries.

Our results represent a significant improvement with respect to those reported in the literature on Cu₆Sn₅ on metal current collectors, particularly in terms of cycling stability over a high number of

cycles.^{15,23} The excellent performance of the Cu₆Sn₅/CP electrodes to repeated lithiation/delithiation processes is due to the CP current collector's characteristics; (i) it is a three-dimensional conductive matrix with micrometric, interconnected carbon fibers which can be homogeneously covered with the electrochemical alloy or host the mechanochemical one without addition of conducting agent (we did not observe differences in performance of electrodes having the same mass loading prepared by the two methods); (ii) it is a light-weight current collector; and (iii) it is more "pliant" than Cu foil so that alloy cracking is less detrimental.

It may also be interesting for materials such as Sn, and work is in progress on this matter.

Acknowledgments

This research was funded by COFIN2002 (Nanostructured alloys as anodes for Li-ion batteries). The authors thank the group of Professor G. Cocco (University of Sassari), partner of the project, for the mechanochemical preparation of the nanometric Cu₆Sn₅ alloy and Dr. R. Berti (Department of Physics, University of Bologna) for useful suggestions in the SEM and EDS analyses.

The University of Bologna assisted in meeting the publication costs of this article.

References

1. J.-M. Tarascon and M. Armand, *Nature (London)*, **414**, 359 (2001).
2. M. Noel and V. Suryanarayanan, *J. Power Sources*, **111**, 193 (2002).
3. J. S. Gnanaraj, M. D. Levi, E. Levi, G. Salitra, D. Aurbach, J. E. Fisher, and A. Claye, *J. Electrochem. Soc.*, **148**, A525 (2001).
4. J. Yao, G. X. Wang, J. Ahn, H. K. Liu, and S. X. Dou, *J. Power Sources*, **114**, 292 (2002).
5. S. Hossain, Y.-K. Kim, Y. Saleh, and R. Loutfy, *J. Power Sources*, **114**, 264 (2002).
6. Y. Idota, T. Kubota, A. Matsufuji, Y. Maekawa, and T. Miyasaka, *Science*, **276**, 1395 (1997).
7. S. Grugeon, S. Laruelle, L. Dupont, and J.-M. Tarascon, *Solid State Ionics*, **5**, 895 (2003).
8. M. Winter and J. O. Besenhard, *Electrochim. Acta*, **45**, 31 (1999).
9. J. Yang, M. Winter, and J. O. Besenhard, *Solid State Ionics*, **90**, 281 (1996).
10. W. X. Chen, J. Y. Lee, and Z. Liu, *Electrochem. Commun.*, **4**, 260 (2002).
11. Y. Liu, J. Y. Xie, Y. Takeda, and J. Yang, *J. Appl. Electrochem.*, **32**, 687 (2002).
12. Y. Liu, J. Y. Xie, and J. Yang, *J. Power Sources*, **119-121**, 572 (2003).
13. N. Tamura, R. Ohshita, M. Fujimoto, M. Kamino, and S. Fujitani, *J. Electrochem. Soc.*, **150**, A679 (2003).
14. J. Wolfenstine, S. Campos, D. Foster, J. Read, and W. K. Behl, *J. Power Sources*, **109**, 230 (2002).
15. S. D. Beattie and J. R. Dahn, *J. Electrochem. Soc.*, **150**, A894 (2003).
16. J. Yang, Y. Takeda, N. Imanishi, T. Ichikawa, and O. Yamamoto, *J. Power Sources*, **79**, 220 (1999).
17. K. Zaghib, X. Song, A. Guerfi, R. Kostecki, and K. Kinoshita, in *New Trends in Intercalation Compounds for Energy Storage Conversion*, K. Zaghib, C. M. Julien, and J. Prakash, Editors, PV 2004-20, p. 29, The Electrochemical Society Proceedings Series, Pennington, NJ (2004).
18. N. Li, D. T. Mitchell, K.-P. Lee, and C. R. Martin, *J. Electrochem. Soc.*, **150**, A979 (2003).
19. S. Fujitani, H. Yagi, K. Sayama, T. Yoshida, and H. Tarui, Abstract 1152, The Electrochemical Society Meeting Abstracts, Paris, France, April 27-May 2, 2003.
20. D. Larcher, L. Y. Beaulieu, D. D. MacNeil, and J. R. Dahn, *J. Electrochem. Soc.*, **147**, 1658 (2000).
21. L. Y. Beaulieu, S. D. Beattie, T. D. Hatchard, and J. R. Dahn, *J. Electrochem. Soc.*, **150**, A419 (2003).
22. L. M. L. Fransson, J. T. Vaughney, K. Edstrom, and M. M. Thackeray, *J. Electrochem. Soc.*, **150**, A86 (2003).
23. M. M. Thackeray, J. T. Vaughney, C. S. Johnson, A. J. Kropf, R. Benedek, L. M. L. Fransson, and K. Edstrom, *J. Power Sources*, **113**, 124 (2003).
24. K. D. Kepler, J. T. Vaughney, and M. M. Thackeray, *Electrochem. Solid-State Lett.*, **2**, 307 (1999).
25. B. A. Johnson and R. E. White, *J. Power Sources*, **70**, 48 (1998).
26. R. Moshkev and B. Johnson, *J. Power Sources*, **91**, 86 (2000).